# Chapter 2

# Charmonium - a Theoretical Background

## 2.1 The Quark Model and the Origins of QCD

The quark model as a description of the fundamental structure of hadrons is approximately 35 years old. The existence of quarks was first proposed by M. Gell-Mann [3] and G. Zweig [4] in 1964 to explain the classification of hadrons in terms of the SU(3) symmetry group. In the 'eight-fold way' of Gell-Mann, [5], the SU(3) arrangements of light hadrons were realized. The octets of scalar mesons ($J^P = 0^-$) and the octet (of $J = 1/2$) and decuplet (of $J = 3/2$) baryons were well established, even though the reason for their relationship was not understood. (See Fig. 2.1) The quark model provided the required insight.

The quark model explained the SU(3) symmetry of strangeness and isospin by the SU(3) of three flavors of quarks - the *up*, *down* and *strange* quarks. It explained the meson and baryon octets perfectly, but ran into problems with the baryon decuplet, (see Fig. 2.1) whose corner members had to have three identical quarks (*ddd* for

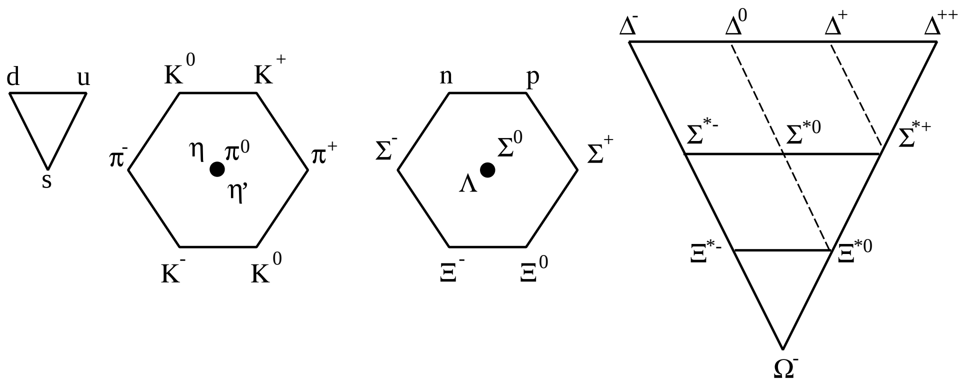


Figure 2.1: SU(3) classification of light quarks, and of hadrons into a $J^P = 0^-$ meson nonet, a spin-1/2 baryon octet, and a spin-3/2 baryon decuplet.

$\Delta^-$, $uuu$ for $\Delta^{++}$, and $sss$ for $\Omega^-$) in relative s-states. This is, of course, forbidden by the generalized Pauli principle. The problem turned out to provide the most important insight into the quark model - one which transformed the quark model into QCD. The quarks needed another quantum number.

Greenberg called it parastatistics, [6] but it was Gell-Mann's name for it, "color charge", that stuck. [7] Quarks were assigned three colors - *red*, *blue* and *green*, and only color neutral (white) objects were allowed to exist in nature. The interaction between quarks is mediated by gluons ($g$). Gluons carry both color and anticolor (i.e. there is an octet of gluons, which reflects the SU(3) symmetry of color). Gluons can therefore interact not only with colored quarks, but also with other gluons.

We therefore have quark-antiquark mesons ($q\bar{q}$ - the quark color is balanced by the antiquark's anticolor) and 3-quark baryons ($qqq$, with one of each color, so that the sum is neutral). Other color-neutral objects are possible, as well: glueballs (2 or 3 gluons, in a color-neutral state), hybrids ($q\bar{q}g$) or multiquark states ($q\bar{q} \cdot q\bar{q}$).

These are known collectively as exotic mesons, and some recent experiments have shown strong evidence for the existence of these states. [8, 9]

### A charming idea - a fourth quark?

Even after the introduction of color, the quark model was not entirely satisfying. Some even found it aestheticially unpleasing. The lepton sector, was known to be organized into two doublets $(e, \nu_e)$ and $(\mu, \nu_\mu)$, but for quarks, one had only a doublet of $(u, d)$ quarks, and a singlet $s$ quark. This observation in part led Bjorken and Glashow [10] to propose a fourth, "up-like" partner to fill the "empty" spot in the strange quark's doublet. Another expectation for a fourth quark, based on more physical considerations, was offered by Glashow, Iliopoulos and Maiani. [11] They proposed a fourth quark to explain some anomalies in the decays of kaons, which were inexplicable in the 3-quark picture.

These predictions were confirmed by experiment in the now-famous "November Revolution" of 1974, which heralded the discovery of $J/\psi$, a narrow resonance with a mass of $\sim$ 3.1 GeV. Very soon after the discovery of $J/\psi$, T. Appelquist and H. D. Politzer [12] speculated that $J/\psi$ might represent the bound state bound state of a fourth quark (charm) and its antiquark, which was qualitatively similar to positronium, the bound state of a positron and an electron. Further, they postulated the existence of several other positronium-like bound states of the charm quark and antiquark. The expected resemblance to positronium led to the whimsical designation of the expected system as charm-onium. Later investigations at SLAC revealed just such a rich spectrum of hidden charm states. The spectra of both positronium and charmonium are displayed in Fig. 2.2.

In the figure, the states are labelled by their quantum numbers ($J^{PC}$), the total angular momentum (J), parity (P) and charge conjugation (C). These are related to the total spin S and the orbital angular momentum L of the system as follows:

$$J = L + S, \quad P = (-1)^{L+1}, \quad \text{and } C = (-1)^{L+S}. \tag{2.1}$$

The states are also designated by the spectroscopic notation $n^{2S+1}L_J$, (where the values of $L = 0, 1, 2...$ are denoted by the letters $S,\ P,\ D...$) so that the $J^{PC} = 0^{-+}$ ground state is written as $1^1S_0$, and its first radial excitation as $2^1S_0$. In addition, the states of charmonium have acquired popular names, some based on analogy with states of lighter quarks ($\eta_c$, $\eta_c'$ for $^1S_0$, and $h_c$ for $^1P_1$), and some based purely on the rights of discovery ($J/\psi$, $\psi'$ for $^3S_1$, and $\chi_J$ for $^3P_J$).

## 2.2 Potential Models for the Strong Interaction

The similarity of positronium and charmonium spectra is quite striking. It was a natural next step after the discovery of charmonium to attempt to model the system as a strongly-interacting analog of positronium. The development of potential models for the strong interaction thus arose from the investigation of the charmonium spectrum. Several of these, including the Cornell potential, [13] Richardson potential, [14] and even some less physically-motivated models taking the form of power law or logarithmic potentials [15] all do a reasonably good job of reproducing the level spacing of the charmonium spectrum. Most notable among these is the

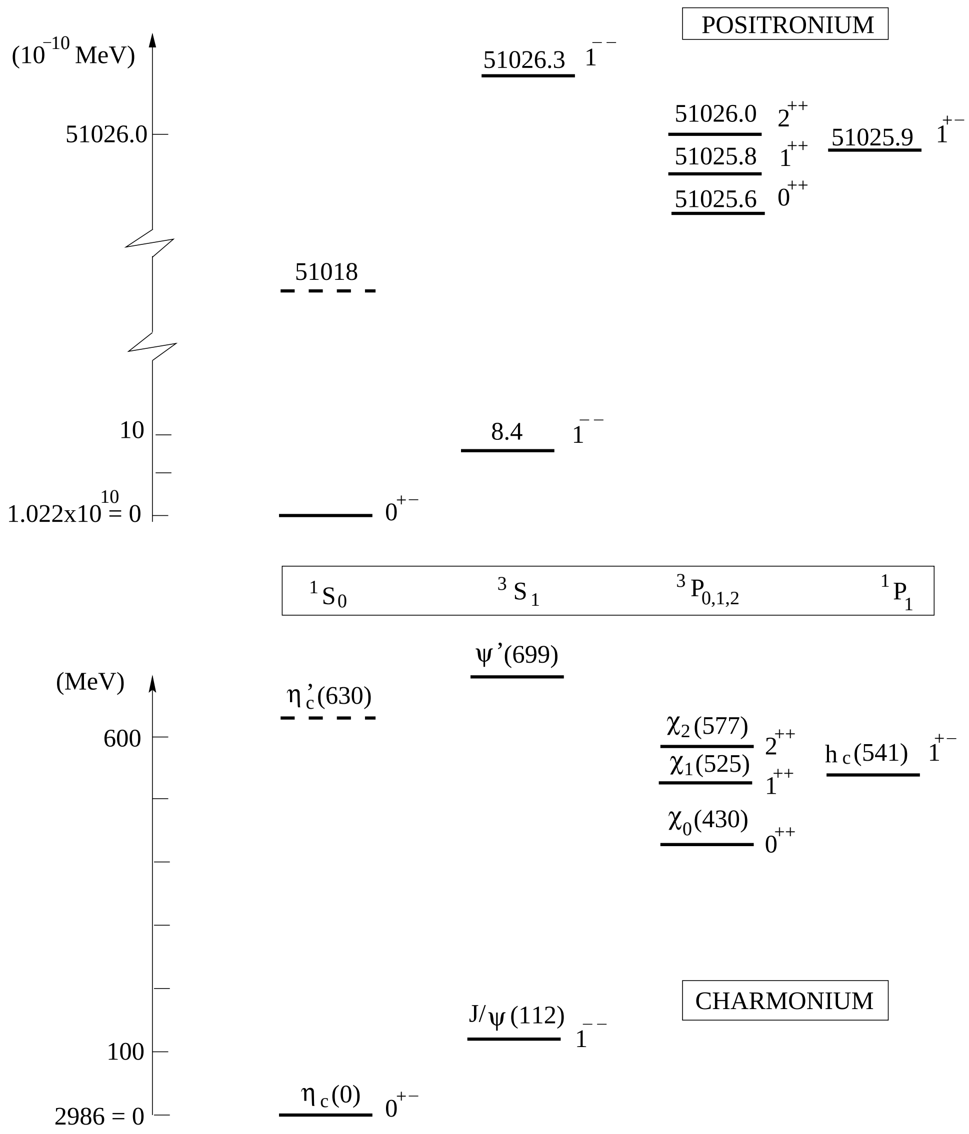


Figure 2.2: A schematic showing the similarities between positronium (top) and charmonium (bottom) spectra.

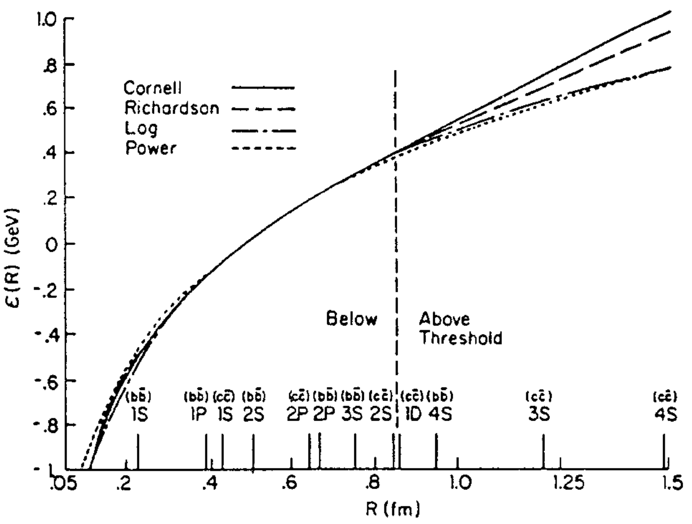


Figure 2.3: Schematic showing various model potentials as a function of quark separation distance $R$. Various $c\bar{c}$ and $b\bar{b}$ levels are indicated by the vertical lines.

Cornell Potential [13],

$$V(r) = -\frac{4}{3}\frac{\alpha_{\mathrm{S}}}{r} + kr. \tag{2.2}$$

The first term in the potential should be immediately recognized as Coulombic in nature, analogous to the QED potential. It corresponds to the exchange of a single massless gluon. $\alpha_{\mathrm{S}}$ is the strong coupling constant, and plays the same role in QCD as $\alpha_{\mathrm{EM}}$ does in QED. The second term is the so-called "confinement" term, and reflects the fact that we observe no free quarks in nature. It is often ascribed to the exchange of multiple gluons, and thought of as a "flux tube", or a "string".

For short distances $r$, the Coulombic term is dominant. The smaller the "size" of a meson, the more Coulomb-like is the interaction between its constituents. Thus the low-lying states of charmonium resemble those of positronium, while the higher states may very well reflect significant perturbations due to the confinement potential.

The spin dependence of the quark-antiquark interactions is important for the description of structure in the charmonium spectrum. These interactions depend on the Lorentz nature (scalar or vector exchange) of the strong interaction. The Coulomb-like part of the potential is believed to be dominantly vector, since it is presumed to arise from the exchange of a single vector gluon. The confinement term can contain either vector or scalar contributions, since it corresponds to multiple-gluon exchange.

Fine structure arises from spin-orbit ($\vec{L} \cdot \vec{S}$) interactions - it can include both vector and scalar contributions. The fine structure in charmonium corresponds to the splitting among the ${}^3P_J$ levels, for example. The hyperfine structure of the charmonium system arises from spin-spin ($\vec{S}_1 \cdot \vec{S}_2$) interactions between the quarks. The hyperfine splitting for $L = 0$ corresponds to the mass difference between the $\eta_c$ and $J/\psi$, and between the $\eta_c'$ and $\psi'$.

Potential models which drew on analogies to positronium are quite successful in describing the gross features of the charmonium spectrum. The early theoretical calculations of decay rates of charmonium states were also made by direct analogy with those for positronium. In the next two sections, we introduce briefly the quantum theories of the interactions which give rise to positronium and charmonium, and present some lowest-order calculations of charmonium decay rates, by analogy with similar calculations for positronium.


Figure 2.4: Feynman diagrams illustrating the basic QED vertex: (left) $e^-$ emitting a photon (right) $e^-$ and $e^+$ annihilating into a photon.

## 2.3 Quantum Electrodynamics and Positronium

Quantum Electrodynamics (QED) is the quantum theory which describes the interaction between electrically charged particles. Electromagnetic interactions may be expressed in terms of the exchange of a photon or photons between the particles in question. The theory of QED reached maturity in the 1940's and 1950's, on the basis of work by Feynman, Schwinger and Tomonaga [16], for which the three jointly received the 1965 Nobel prize.

The basic QED vertex is represented by the Feynman diagrams shown in Fig. 2.4. Time in the diagrams flows from left to right: fermions have arrows which point to the right, while antifermions have arrows pointing to the left. The diagram on the left shows a fermion (here, an electron) entering the diagram, emitting a photon, and leaving. The diagram on the right shows an electron and positron pair annihilating, producing a single photon.

These diagrams illustrate the basic vertex only; neither diagram is allowed kinematically as drawn. In order to emit a photon as in the diagram on the left in

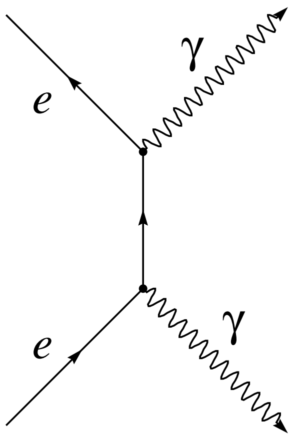


Figure 2.5: The two contributing Feynman diagrams for the 2-photon annihilation process $e^+e^-\to\gamma\gamma$

Figure 2.4, the electron must interact with an external electric field, or another charged object. The annihilation diagram on the right is also not possible as drawn. An isolated $e^+e^-$ pair cannot annihilate into a single real photon and conserve four-momentum. However, the pair can annihilate into two photons (see Figure 2.5). The calculation for this cross section is useful for our discussion, so we outline it here.

Using the rules for Feynman diagrams, we may calculate the cross section for this reaction. The two diagrams in Fig. 2.5 contribute

$$g_e^2\bar{v}_2\left(\not{k}_4\frac{(\not{p}_1-\not{p}_3)+mc}{(p_1-p_3)^2-m^2c^2}\not{k}_3+\not{k}_3\frac{(\not{p}_1-\not{p}_4)+mc}{(p_1-p_4)^2-m^2c^2}\not{k}_4\right)u_1 \tag{2.3}$$

to the matrix element $\mathcal{M}$, using the notation of Bjorken and Drell. [17] Using the Dirac equation, $(\not{p}_1-mc)u_1=0$, and the rules for permuation of Dirac matrices, this simplifies to

$$\mathcal{M} = -g_e^2 \bar{v}_2 \left( \frac{\not{\epsilon}_4 \not{p}_3 \not{\epsilon}_3}{2p_1p_3} + \frac{\not{\epsilon}_3 \not{p}_4 \not{\epsilon}_4}{2p_1p_4} \right) u_1 \tag{2.4}$$

in the reference frame in which positron has energy E and the electron is at rest (This is used for simplicity of calculation; the result is in fact frame independent) and in the Coulomb or transverse gauge (so that $(\vec{p}_1 \cdot \epsilon_3) = (\vec{p}_1 \cdot \epsilon_4) = 0$).

We can then calculate the differential cross section by inserting this expression into a general formula for a two-body process $1 + 2 \rightarrow 3 + 4$:

$$d\sigma = \int \frac{d^3p_3}{2p_3} \int \frac{d^3p_4}{2p_4} (2\pi)^4 \delta(p_3 + p_4 - p_1 - p_2) \frac{1}{v_{12}} \frac{m^2}{E_1 E_2} |\mathcal{M}|^2 \tag{2.5}$$

For unpolarized initial and final states, we need to average over initial spins and sum over final polarizations. Thus $|\mathcal{M}|^2$ is replaced by $(1/4) \sum_f |\mathcal{M}|^2$:

$$\begin{aligned} d\sigma = & \frac{e^4}{16\pi^2} \frac{m}{E\beta} \int \frac{d^3p_3}{2p_3} \int \frac{d^3p_4}{2p_4} \delta(p_3 + p_4 - p_1 - p_2) \\ & \times Tr \frac{\not{p}_1 - m}{2m} \left( \frac{\not{\epsilon}_4 \not{p}_3 \not{\epsilon}_3}{2p_1p_3} + \frac{\not{\epsilon}_3 \not{p}_4 \not{\epsilon}_4}{2p_1p_4} \right) \frac{\not{p}_2 - m}{2m} \left( \frac{\not{\epsilon}_3 \not{p}_3 \not{\epsilon}_4}{2p_1p_3} + \frac{\not{\epsilon}_4 \not{p}_4 \not{\epsilon}_3}{2p_1p_4} \right) \end{aligned} \tag{2.6}$$

Using the rules for evaluation of the traces, [17] and performing the phase space integrals to find the total cross section $\sigma$, we obtain, in the non-relativistic limit,

$$\sigma(e^+e^- \rightarrow \gamma\gamma) = \frac{4\pi}{\beta} \left( \frac{\alpha_{\rm EM}}{m_e} \right)^2 . \tag{2.7}$$

### 2.3.1 Application of QED to positronium decays

The ground state of positronium is the $1^1S_0$ state. Since there are no fermions lighter than electrons, positronium can only decay by annihilation into photons. No positronium state can decay into a single photon, because that would violate four-momentum conservation. The $^1S_0$ state therefore decays into two photons. This decay is forbidden to the $^3S_1$ state by Yang's theorem, [19] so the $^3S_1$ state can only decay into three photons. We can use the calculation of $\sigma(e^+e^-\!\rightarrow\!\gamma\gamma)$ to calculate the two-photon decay rate of the positronium state.

The cross section result in Eq. 2.7 can be converted to a width for the annihilation of $^1S_0$ positronium by multiplying it by the probability that the electron and positron are at the origin ($|\psi(0)|^2$, the square of the wave function at the origin) and by $\beta$, where $\beta$ is the velocity of the electron or positron in the center of mass frame. We can thus express the width for annihilation of the singlet ($^1S_0$) state to lowest order as:

$$\Gamma(^1S_0\!\rightarrow\!\gamma\gamma) = \frac{4\pi}{\beta}\left(\frac{\alpha_{\text{EM}}}{m_e}\right)^2 \times \beta|\psi(0)|^2 = \frac{4\pi{\alpha_{\text{EM}}}^2}{m_e^2}|\psi(0)|^2 \tag{2.8}$$

For hydrogen, $|\psi(0)|^2$ is well known from elementary quantum mechanics. The positronium 1S wave function is identical to that of hydrogen, except for a difference in length scale. The Bohr radius of the hydrogen atom, which is defined as the mean distance of the electron from the proton, is given by $a = 1/(\alpha_{\text{EM}}m_e)$. In the case of positronium, $m_e$ must be replaced by the reduced mass $\mu$, where $\mu = (m_e)(m_e)/(m_e\!+\!m_e) = (1/2)m_e$. Thus, the Bohr radius of positronium has the value $a_{pos} = 1/(\alpha_{\text{EM}}\mu) = 2/(\alpha_{\text{EM}}m_e)$, or twice that of hydrogen.

So, the positronium 1S wave function at the origin is equivalent to that of hydrogen ($\psi(0) = \sqrt{(8\pi/a^3)}$), but with the replacement of the Bohr radius $a$ with $2a$:

$$|\psi(0)|^2 = \frac{1}{\pi a^3} = \frac{1}{\pi}\left(\frac{e^2 m_e}{8\pi}\right)^3. \tag{2.9}$$

Therefore,

$$\Gamma(^1S_0 \to \gamma\gamma) = 4\pi \left(\frac{\alpha_{\text{EM}}}{m_e}\right)^2 \frac{m_e^3 e^6}{8^3 \pi^3} = \frac{\alpha_{\text{EM}}{}^2}{2^8} \frac{m_e e^6}{\pi^2 \hbar^4} = \frac{1}{2} \alpha_{\text{EM}}{}^5 \pi m_e. \tag{2.10}$$

The lifetime of the state, $\tau = \hbar/\Gamma$, is

$$\tau = 1.2449 \times 10^{-10}\ sec. \tag{2.11}$$

First and second order QED radiative corrections give: [20]

$$\Gamma(^1S_0 \to \gamma\gamma) = \frac{\alpha_{\text{EM}}{}^5 \pi m_e c^2}{2\hbar} \left(1 - \frac{\alpha_{\text{EM}}}{\pi}(5 - \frac{\pi^2}{4}) - 2\alpha_{\text{EM}}{}^2 ln(\alpha_{\text{EM}})\right). \tag{2.12}$$

which modifies the lifetime prediction to:

$$\tau = 1.2516 \times 10^{-10}\ sec. \tag{2.13}$$

(Notice that the first order radiative correction, $\sim 0.8\alpha_{\text{EM}}$, amounts to only $\approx 0.6\%$, because of the small value of $\alpha_{\text{EM}} = 1/137$.)

Experimentally, the lifetime of the $^1S_0$ ground state of positronium is [21]:

$$\tau = 1.2515 \pm 0.0003 \times 10^{-10}\ sec, \tag{2.14}$$

which is in very good agreement with the QED prediction.

## 2.4 Quantum Chromodynamics

Quantum Chromodynamics (QCD) is the theory which has been developed over the past three decades to describe the strong interaction as a quantum field theory.

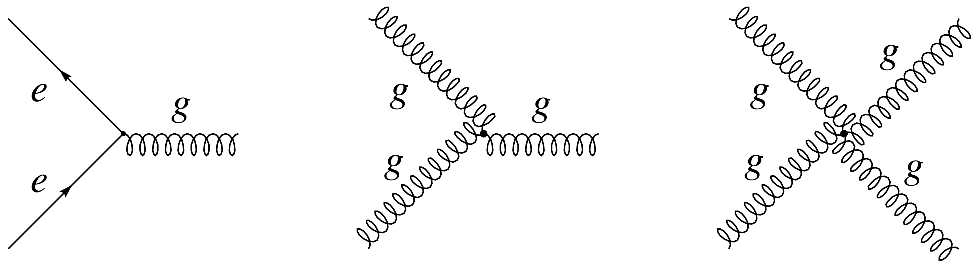


Figure 2.6: The three basic QCD vertices.

It is not nearly as transparent as QED, partly because it is mathematically more intricate. It is nonetheless quite successful in describing the basic hadronic structures we observe.

Since the mediator of QCD, the gluon, can interact not only with quarks, but with other gluons, there are three basic vertices in QCD (*c.f.* QED's single elementary vertex) and these are shown in Fig. 2.6. Ultimately, this gluon self-interaction manifests itself in the two phenomena we know as confinement and asymptotic freedom.

## 2.5 Application of QED and QCD to charmonium decays

We discuss two types of processes involving charmonium in this dissertation. Each of the states investigated in this work couples to two photons, and similarly to two gluons. We can arrive at estimates for the partial widths of $c\bar{c}\to\gamma\gamma$ and $c\bar{c}\to gg$, using the result of the calculation of the $e^+e^-\to\gamma\gamma$ cross section presented in Sec. 2.3.

For instance, by replacing the coupling constant $\alpha_{\text{EM}}$ in Equation 2.8 by the appropriate value for the charm quark, $(\frac{2}{3})^2 \times \alpha_{\rm EM} = \frac{4}{9}\alpha_{\rm EM}$, and $m_e$ by $m_c$, and multiplying by 3 (for the 3 possible color combinations allowed for the charmonium system) we arrive at a lowest order estimate of $\Gamma(c\bar{c}(^1S_0)\to\gamma\gamma)$:

$$\Gamma(c\bar{c}(^1S_0)\to\gamma\gamma) = \frac{64\pi{\alpha_{\rm EM}}^2}{27m_c^2}|\psi^S_{c\bar{c}}(0)|^2. \tag{2.15}$$

Since the strong interaction potential isn't *precisely* Coulombic, even at very short range, we cannot assume that the charmonium wave function is a Coulomb wave function, like we did in Equation 2.10. Thus we leave the prediction in terms of the 1S charmonium wave function at the origin $\psi(0)$.

We can estimate the value of the two-gluon annihilation width of $^1S_0$ charmonium in a similar manner as we have the $\gamma\gamma$ width. Assuming that one gluon exchange dominates the charm-anticharm interaction, we can substitute into Eq. 2.8 the strong coupling constant $\alpha_{\rm S}$ for $\alpha_{\rm EM}$, along with the appropriate combinatoric color factor of (9/8), to arrive at the lowest order result for $\Gamma(c\bar{c}(^1S_0)\to gg)$:

$$\Gamma(c\bar{c}(^1S_0)\to gg) = \frac{8\pi}{3}\frac{{\alpha_{\rm S}}^2}{m_c^2}|\psi^S_{c\bar{c}}(0)|^2 \tag{2.16}$$

Similar, somewhat more complicated calculations can be made for the $\gamma\gamma$ and $gg$ decay rates of the $^3P_2$ and $^3P_0$ states as well.

In the discussion of our results in Chapter 8, we will be interested in comparing the $\gamma\gamma$ partial widths of the $^1S_0$ charmonium states with the leptonic partial widths of the corresponding $^3S_1$ states. The calculation of $\Gamma(^3S_1\to e^+e^-)$ is also a simple QED calculation, following directly from the calculation of cross section for the process $e^+e^-\to\mu^+\mu^-$. The calculation of the leptonic widths of vector mesons was presented in 1967 by Van Royen and Weisskopf [22]. In terms of the mass of the

Table 2.1: First-order partial width predictions and the first order radiative corrections. [23] According to Kwong, *et al.* , the radiative corrections have typical uncertainties of $\pm\alpha_{\rm s}/\pi$, or approximately $\pm 11\%$.

| Partial Width | Lowest order Prediction $\Gamma_0$ | First Order Correction | Correction % $\alpha_{\rm s} = 0.35$ |
|---|---|---|---|
| ${}^1S_0 \to \gamma\gamma$ | $64\pi{\alpha_{\rm EM}}^2 \lvert\psi_S(0)\rvert^2/27m_c^2$ | $1 - 3.4\alpha_{\rm s}/\pi$ | -37.8 |
| ${}^1S_0 \to gg$ | $8\pi{\alpha_{\rm s}}^2 \lvert\psi_S(0)\rvert^2/3m_c^2$ | $1 + 4.8\alpha_{\rm s}/\pi$ | 53.5 |
| ${}^3S_1 \to e^+e^-$ | $64{\alpha_{\rm EM}}^2 \lvert\psi_S(0)\rvert^2/9M^2$ | $1 - 5.3\alpha_{\rm s}/\pi$ | -59.0 |
| ${}^3P_0 \to \gamma\gamma$ | $16{\alpha_{\rm EM}}^2 \lvert R'_P(0)\rvert^2/3m_c^4$ | $1 + 0.2\alpha_{\rm s}/\pi$ | 2.2 |
| ${}^3P_0 \to gg$ | $6{\alpha_{\rm s}}^2 \lvert R'_P(0)\rvert^2/m_c^4$ | $1 + 9.5\alpha_{\rm s}/\pi$ | 105.8 |
| ${}^3P_2 \to \gamma\gamma$ | $64{\alpha_{\rm EM}}^2 \lvert R'_P(0)\rvert^2/45m_c^4$ | $1 - 5.3\alpha_{\rm s}/\pi$ | -59.0 |
| ${}^3P_2 \to gg$ | $8{\alpha_{\rm s}}^2 \lvert R'_P(0)\rvert^2/5m_c^4$ | $1 - 2.2\alpha_{\rm s}/\pi$ | -24.5 |

vector state $M_V$, and the wave function at the origin $\psi(0)$, the leptonic decay rate for vector charmonia is given by:

$$\Gamma(c\bar{c}({}^3S_1) \to l^+l^-) = \frac{64\pi\alpha_{\rm EM}}{9M_V^2}|\psi(0)|^2. \tag{2.17}$$

First order QCD radiative corrections have been made to all these partial width predictions, and are summarized in Ref. [23]. Each of the corrected widths has the form $\Gamma = \Gamma_0 \times (1 + B\alpha_{\rm s})$, where $\Gamma_0$ is the lowest order partial width prediction. These partial width predictions and their first-order radiative corrections are presented in Table 2.1. We note that because of the largeness of the strong coupling constant $\alpha_{\rm s}$, ($\approx 0.35$ in the charmonium region) the first order radiative corrections are large ($20\% - 100\%$), raising serious questions about their validity.

The formulae in the Table 2.1 are not very useful in making absolute width predictions, because of the presence of several unknown quantities. In all cases, $\alpha_{\mathrm{s}}$ and $m_c$ appear, as well as the total wavefunctions $|\psi_S(0)|^2$ or the radial wave function derivatives $|R'_P(0)|^2$ at the origin. All of these are unknown, so the best practical use of these width predictions is in terms of their ratios, constructed so as to cancel $m_c$ as well as $|\psi_S(0)|^2$ or $|R'_P(0)|^2$. These ratios can then be used to determine values of $\alpha_{\mathrm{s}}(m_c)$ from the experimental data. We will present such an analysis in Chapter 8, using our data taken at $\eta_c$ and $\chi_2$, and appropriate ratios constructed from the partial widths in the above table.